Robust Passive Piezoelectric Shunt Dampener

S. Behrens, A. J. Fleming and S. O. R. Moheimani

School of Electrical Engineering and Computer Science
University of Newcastle NSW 2308 Australia

ABSTRACT

This paper introduces a new multiple mode passive piezoelectric shunt damping technique. The robust passive piezoelectric shunt controller is capable of damping multiple structural modes and maybe less susceptible to variations in environmental conditions that can severely e¤ect the performance of other controllers. The proposed control scheme is validated experimentally on a piezoelectric laminated plate structure.

Keywords: robust, multiple mode, adaptive, piezoelectric shunt, vibration damping.

1. INTRODUCTION

Placing an electrical impedance across the terminals of a piezoelectric transducer, adhered to a ‡exible mechanical structure, with the view to minimizing structural vibrations, is referred to as piezoelectric shunt damping.[1{5] This technique has been proven to be a reliable alternative to active piezoelectric vibration control techniques,[6, 7] o¤ering the bene…ts of stability and performance without the need for additional sensors. Most importantly, the inherent robustness makes passive shunt control techniques very desirable.

Passive piezoelectric shunt damping[2, 4, 8{10] consists of an electrical network of passive components e.g. capacitors, inductors and resistors. Most passive schemes act to minimize structural vibration at a particular frequency, normally associated with a lightly damped vibration mode. These frequencies are rarely stationary in real applications. For example, changes in climatic conditions may shift resonance frequencies of the structure. Some damping is usually added to ensure e¤ectiveness over a range of frequencies.

Authors, Hollkamp et. al.,[11] Sun et. al.,[12] von Flotow et. al.[13] and Fleming et. al.,[14] present methods for tracking the structural frequencies of the lightly damped system. The passive shunt is adaptively tuned to account for the changing environmental conditions. One disadvantage with these techniques is the additional processing power of the digital signal processor (DSP).

This paper proposes a new method for passive shunt damping. The robust passive piezoelectric shunt controller is robust, passive and is capable of damping multiple modes. In addition, it maybe less susceptible to environmental conditions than comparable techniques.

The remainder of the paper continues as follows. Section 2 is concerned with the piezoelectric shunt damping problem and the speci…c feedback structure associated with it. Section 3 introduces a class of robust passive piezoelectric shunt controllers that can be e¤ective in reducing vibration of a ‡exible structure. Section 4 summarizes our experimental results, and Section 5 concludes the paper.

2. PIEZOELECTRIC SHUNT DAMPING FEEDBACK STRUCTURE

Consider the system depicted in Figure 1, in which a piezoelectric transducer is attached to the surface of a ‡exible structure using strong adhesive material. The piezoelectric transducer is shunted by an electrical impedance Z. As the structure deforms, possibly due to a disturbance w, an electric charge distribution develops inside the piezoelectric transducer. The transducer can be thought of as a parallel plate capacitor, with a capacitance of C_p, and a linear strain dependent voltage source v_p.[2, 6, 15{17] The electric charge will result in a voltage di¤erence v across the conducting surfaces of the piezoelectric transducer which in turn results in the ‡ow of electric current i through the impedance.

Corresponding author: S. Behrens: E-mail: sbehrens@ecemail.newcastle.edu.au; Telephone: +61 2 4921 7223. Fax: +61 2 4921 7058.

In this section the piezoelectric shunt feedback structure is explained. For more details refer to.[18] According to Ohm's law,

$$v(s) = i(s)Z(s). \tag{1}$$

Furthermore, by writing Kirchhoff's voltage law for the shunted transducer, as shown in Figure 1 (b), we obtain

$$v(s) = v_p(s) - \frac{1}{C_p s} i. \tag{2}$$

Now, assuming that the structure is disturbed by a voltage v_{in}, which is applied to the actuating layer, as shown in Figure 1, and impedance is attached to piezoelectric terminals, then the overall linear relationship is

$$v_p(s) = G_{vv}(s)v_{in}(s) - G_{vv}(s)v(s). \tag{3}$$

$G_{vv}(s)$ is the collocated dynamics between the open circuit shunting voltage, $v(s)$ or $v_p(s)$, and the disturbance voltage $v_{in}(s)$. We can write the transfer function $G_{vv}(s)$, as

$$G_{vv}(s) \triangleq \frac{v(s)}{v_{in}(s)} = \sum_{i=1} \frac{f_i}{s^2 + 2\zeta_i \omega_i s + \omega_i^2}, \tag{4}$$

where ζ_i is the structural damping, ω_i is the resonant frequencies of the mechanical structure. Also, note that the gain f_i is dependent on the properties of the flexible structure and piezoelectric transducers.

By combining (1), (2) and (3), we obtain the following damped system

$$\tilde{G}_{vv}(s) \triangleq \frac{v_p(s)}{v_{in}(s)} = \frac{G_{vv}(s)}{1 + \frac{Z(s)C_p s}{Z(s)C_p s+1} G_{vv}(s)}. \tag{5}$$

From equation (5) the transfer function relating $v_p(s)$ and $v_{in}(s)$, is the feedback connection of $G_{vv}(s)$ with

$$K(s) = \frac{Z(s)C_p s}{Z(s)C_p s + 1}. \tag{6}$$

This is an interesting observation as it enables one to employ theoretical tools to analyze the dynamics of the shunted system. The feedback control problem associated with (5) is illustrated in Figure 2. Note the inner feedback structure loop which represents the effective controller $K(s)$ in (6). Observe that the purpose of the control system is to regulate $v_p(s)$, in the presence of a disturbance $v_{in}(s)$.

The above system is used mainly for laboratory experiments. For a more realistic environment, the disturbance acting on the flexible structure may have some type of spatial disturbance. For example, point force(s), moment(s) and pressure force(s), or a combination of the above disturbances. In this situation, equation (3) should be modified to

$$v_p(s) = G_{vv}(s)v_{in}(s) - G_{vw}(s)w(s), \tag{7}$$

where $G_{vw}(s)$ is the undamped transfer function from the disturbance vector, $w(s)$ to $v_p(s)$. In this case, the shunted dynamics (7) are modified to

$$\tilde{G}_{vw}(s) \triangleq \frac{v_p(s)}{w(s)} = \frac{G_{vw}(s)}{1 + K(s)G_{vv}(s)}, \tag{8}$$

and

$$G_{vw}(s) = \sum_{i=1} \frac{\hat{f}_i}{s^2 + 2\zeta_i \omega_i s + \omega_i^2}, \tag{9}$$

where the gain $\hat{f}_i$ is dependent on the piezoelectric transducer, flexible structure and applied disturbance.

Observe that the nature of the disturbance has changed, but the shunted system is still characterized by the feedback connection of $G_{vv}(s)$ and $K(s)$. Therefore, the feedback system depicted in Figure 2 should be modified to that shown in Figure 3.

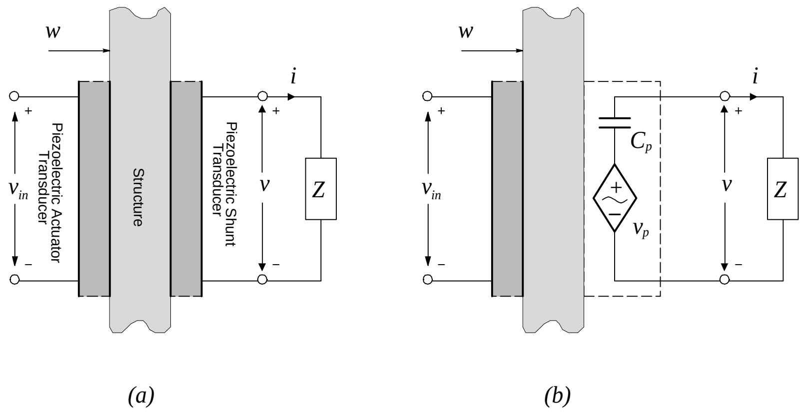

Figure 1. (a) Structure with collocated piezoelectric transducers, and (b) equivalent circuit schematic of the shunted system.

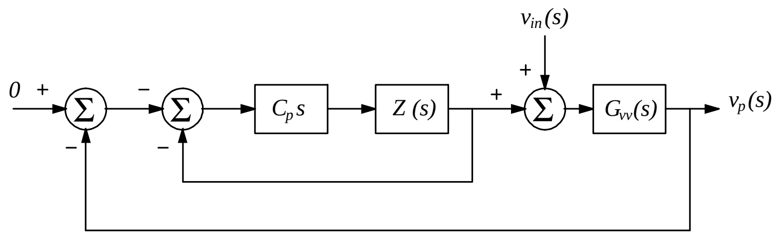

Figure 2: The feedback structure associated with shunt damping.

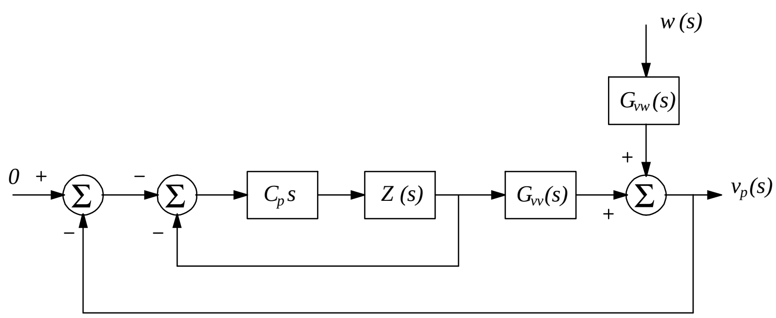

Figure 3: The feedback structure associated with the modi…ed shunt damping.

3. DEVELOPING ROBUST PASSIVE PIEZOELECTRIC SHUNT CONTROLLER

In the previous section, we demonstrated that piezoelectric shunt damping can be viewed as a feedback control problem of a specific structure. Using this underlying structure, we can design an impedance Z that moves the damped poles of the shunted system deeper into the left half plane, i.e. to add more damping.

Two effective impedances for this purpose were developed by Moheimani et. al..[18, 19] They are

$$Z_1(s) = \frac{1 - \sum_{i=1}^{N} \frac{\alpha_i \tilde{\omega}_i^2}{s^2+2\tilde{\zeta}_i\tilde{\omega}_i s+\tilde{\omega}_i^2}}{C_p s \sum_{i=1}^{N} \frac{\alpha_i \tilde{\omega}_i^2}{s^2+2\tilde{\zeta}_i\tilde{\omega}_i s+\tilde{\omega}_i^2}} = \frac{\sum_{i=1}^{N} \left(s + 2\tilde{\zeta}_i\tilde{\omega}_i\right) \prod_{l=1;i\neq l}^{N} \left(s^2 + 2\tilde{\zeta}_l\tilde{\omega}_l s + \tilde{\omega}_l^2\right)}{C_p \sum_{i=1}^{N} \left[\alpha_i \tilde{\omega}_i^2\right] \prod_{l=1;i\neq l}^{N} \left(s^2 + 2\tilde{\zeta}_l\tilde{\omega}_l s + \tilde{\omega}_l^2\right)} \tag{10}$$

$$Z_2(s) = \frac{1 - \sum_{i=1}^{N} \frac{\alpha_i (2\tilde{\zeta}_i\tilde{\omega}_i s+\tilde{\omega}_i^2)}{s^2+2\tilde{\zeta}_i\tilde{\omega}_i s+\tilde{\omega}_i^2}}{C_p s \sum_{i=1}^{N} \frac{\alpha_i (2\tilde{\zeta}_i\tilde{\omega}_i s+\tilde{\omega}_i^2)}{s^2+2\tilde{\zeta}_i\tilde{\omega}_i s+\tilde{\omega}_i^2}} = \frac{\sum_{i=1}^{N} (\alpha_i s) \prod_{l=1;i\neq l}^{N} \left(s^2 + 2\tilde{\zeta}_l\tilde{\omega}_l s + \tilde{\omega}_l^2\right)}{C_p \sum_{i=1}^{N} \alpha_i \left(2\tilde{\zeta}_i\tilde{\omega}_i s + \tilde{\omega}_i^2\right) \prod_{l=1;i\neq l}^{N} \left(s^2 + 2\tilde{\zeta}_l\tilde{\omega}_l s + \tilde{\omega}_l^2\right)} \tag{11}$$

where $\tilde{\omega}_i$ is the specified frequencies and the damping parameter $\tilde{\zeta}_i$, must satisfy $\tilde{\zeta}_i > 0$ for $i = 1; 2; 3; \ldots; N$. Also, for passivity the following condition must be satisfied

$$\sum_{i=1}^{N} \alpha_i = 1 \text{ and } \alpha_i > 0. \tag{12}$$

An immediate choice for is $\alpha_i = \frac{1}{N}$ for $i = 1; 2; 3; \ldots; N$.

It is straightforward to verify that for the impedances $Z_1(s)$ and $Z_2(s)$, the effective controllers $K(s)$ in equation (6) will be[18, 19]

$$K_1(s) = \sum_{i=1}^{N} \frac{\alpha_i s \left(s + 2\tilde{\zeta}_i\tilde{\omega}_i\right)}{s^2 + 2\tilde{\zeta}_i\tilde{\omega}_i s + \tilde{\omega}_i^2}; \tag{13}$$

and

$$K_2(s) = \sum_{i=1}^{N} \frac{\alpha_i s^2}{s^2 + 2\tilde{\zeta}_i\tilde{\omega}_i s + \tilde{\omega}_i^2}. \tag{14}$$

Normally for the proposed impedances, (10) and (11), the frequencies $\tilde{\omega}_i$ are equal to the structural resonance frequencies ω_i, i.e., $\omega_i = \tilde{\omega}_i$. For the proposed robust passive piezoelectric shunt controller, additional controllers are placed above and below ω_i. That is,

$$\omega_i = \{\tilde{\omega}_{i;-M}; \ldots; \tilde{\omega}_{i;-2}; \tilde{\omega}_{i;-1}; \tilde{\omega}_{i;0}; \tilde{\omega}_{i;1}; \tilde{\omega}_{i;2}; \ldots; \tilde{\omega}_{i;M}\} \qquad i \in \{1 \cdots N\}$$

where $\tilde{\omega}_{i;0}$ is equivalent to the specific frequencies, i.e. $\omega_i = \tilde{\omega}_{i;0}$, assuming that

$$\tilde{\omega}_{i;-M} < \ldots < \tilde{\omega}_{i;-2} < \tilde{\omega}_{i;-1} < \tilde{\omega}_{i;0} < \tilde{\omega}_{i;1} < \tilde{\omega}_{i;2} < \ldots < \tilde{\omega}_{i;M} \qquad i \in \{1 \cdots N\};$$

and

$$\tilde{\omega}_{1;x} < \ldots < \tilde{\omega}_{i;x_N} \qquad x_1; \ldots; x_N \in \{-M \cdots M\}.$$

Therefore, the new damping vector is described as

$$d_i = \{\tilde{\zeta}_{i;-M}; \ldots; \tilde{\zeta}_{i;-2}; \tilde{\zeta}_{i;-1}; \tilde{\zeta}_{i;0}; \tilde{\zeta}_{i;1}; \tilde{\zeta}_{i;2}; \ldots; \tilde{\zeta}_{i;M}\} \qquad i \in \{1 \cdots N\};$$

and

$$\{\tilde{\zeta}_{i;-M}; \ldots; \tilde{\zeta}_{i;-2}; \tilde{\zeta}_{i;-1}; \tilde{\zeta}_{i;0}; \tilde{\zeta}_{i;1}; \tilde{\zeta}_{i;2}; \ldots; \tilde{\zeta}_{i;M}\} > 0 \qquad i \in \{1 \cdots N\}.$$

The two new impedances have the following structures

$$Z_1(s) = \frac{1 - \sum_{i=1}^{N} \Psi_1}{C_p s \sum_{i=1}^{N} \Psi_1}; \tag{15}$$

$$\Psi_1 = \left(\sum_{j=-M}^{-1} \frac{\alpha_{i,j}\,\omega_{i,j}^2}{s^2 + 2\hat{d}_{i,j}\omega_{i,j}s + \omega_{i,j}^2} + \frac{\alpha_{i,0}\,\omega_{i,0}^2}{s^2 + 2\hat{d}_{i,0}\omega_{i,0}s + \omega_{i,0}^2} + \sum_{j=1}^{M} \frac{\alpha_{i,j}\,\omega_{i,j}^2}{s^2 + 2\hat{d}_{i,j}\omega_{i,j}s + \omega_{i,j}^2} \right);$$

and

$$Z_2(s) = \frac{1 - \sum_{i=1}^{N} \Psi_2}{C_p s \sum_{i=1}^{N} \Psi_2}; \tag{16}$$

$$\Psi_2 = \left(\sum_{j=-M}^{-1} \frac{\alpha_{i,j}\left(2\hat{d}_{i,j}\omega_{i,j}s + \omega_{i,j}^2\right)}{s^2 + 2\hat{d}_{i,j}\omega_{i,j}s + \omega_{i,j}^2} + \frac{\alpha_{i,0}\left(2\hat{d}_{i,0}\omega_{i,0}s + \omega_{i,0}^2\right)}{s^2 + 2\hat{d}_{i,0}\omega_{i,0}s + \omega_{i,0}^2} + \sum_{j=1}^{M} \frac{\alpha_{i,j}\left(2\hat{d}_{i,j}\omega_{i,j}s + \omega_{i,j}^2\right)}{s^2 + 2\hat{d}_{i,j}\omega_{i,j}s + \omega_{i,j}^2} \right):$$

where the modified condition $\sum_{i=1}^{N} \sum_{i=-M}^{M} \alpha_{i,j} = 1$ and $\alpha_{i,j} > 0$, must be satisfied by both equations (15) and (16).

It can be observed that the proposed robust passive piezoelectric shunt controller has the order $2M + 1$ for each i^{th} mode. The overall impedance/controller order is $N(2M + 1)$. The effective controllers, $K_1(s)$ or $K_2(s)$, are equivalent to

$$K_1(s) = \sum_{i=1}^{N} \left(\sum_{j=-M}^{-1} \frac{\alpha_{i,j}s\left(s + 2\hat{d}_{i,j}\omega_{i,j}\right)}{s^2 + 2\hat{d}_{i,j}\omega_{i,j}s + \omega_{i,j}^2} + \frac{\alpha_{i,0}s\left(s + 2\hat{d}_{i,0}\omega_{i,0}\right)}{s^2 + 2\hat{d}_{i,0}\omega_{i,0}s + \omega_{i,0}^2} + \sum_{j=1}^{M} \frac{\alpha_{i,j}s\left(s + 2\hat{d}_{i,j}\omega_{i,j}\right)}{s^2 + 2\hat{d}_{i,j}\omega_{i,j}s + \omega_{i,j}^2} \right); \tag{17}$$

$$K_2(s) = \sum_{i=1}^{N} \left(\sum_{j=-M}^{-1} \frac{\alpha_{i,j}s^2}{s^2 + 2\hat{d}_{i,j}\omega_{i,j}s + \omega_{i,j}^2} + \frac{\alpha_{i,0}s^2}{s^2 + 2\hat{d}_{i,0}\omega_{i,0}s + \omega_{i,0}^2} + \sum_{j=1}^{M} \frac{\alpha_{i,j}s^2}{s^2 + 2\hat{d}_{i,j}\omega_{i,j}s + \omega_{i,j}^2} \right): \tag{18}$$

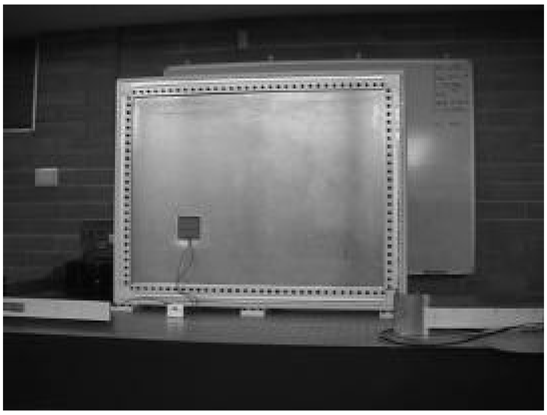

Figure 4: Piezoelectric laminated plate structure.

4. EXPERIMENTAL VALIDATION

The proposed robust passive piezoelectric shunt controller was validated experimentally on a piezoelectric laminated plate structure. A photograph of the structure is shown in Figure 4. Two PIC151 piezoelectric patches are bonded collocated to the aluminum structure using a strong adhesive material. One piezoelectric patch will be used as an actuator (which is visible in Figure 4) to generate a disturbance and the other (which is not visible) as a shunting layer. The measured capacitance of the piezoelectric shunting layer, C_p, is equal to $67.9nF$. For a detailed description of the apparatus, the reader is referred to Behrens et. al..[20]

The first step in the analysis involves procuring a model for the transfer function $G_{vv}(s)$. This allows us to simulate the effect of an attached piezoelectric shunt on the transfer function from the applied actuator voltages $v_{in}(s)$, to the generated piezoelectric shunt layer voltages $v_p(s)$. These variables are internal and cannot be measured directly whilst an impedance is attached to the shunting layer. We will also consider the transfer function from the applied actuator voltages $v_{in}(s)$, to the structural deflection at a point $d(s)$. In our case, we have one input and two outputs, a SIMO system,

$$\begin{bmatrix} v_p(s) \\ d(s) \end{bmatrix} = G(s)v_{in}(s); \qquad (19)$$

where $G(j\omega) \in \mathbb{C}^{2\times1}$ is the open loop plant transfer function matrix, i.e. $G(s) = \begin{bmatrix} G_{vv}(s) \\ G_{dv}(s) \end{bmatrix}$.

System identification can be employed to procure a composite structural-piezoelectric model directly from experimental data. In this paper we employ the algorithm of Van Overschee and De Moor,[21] a continuous time frequency domain subspace method*. The magnitude frequency response of $G(j\omega)$ is plotted in Figure 5. 340 frequency samples from 0 to 300 Hz were used to identify a 6 state model for $G(s)$: The magnitude frequency response of the model is overlaid on the experimental data in Figure 5.

Using a Polytec laser scanning vibrometer (PSV-300) and a Hewlett Packard spectrum analyzer (35670A), the frequency responses for $G_{vv}(s)$ and $G_{dv}(s)$ were obtained. Using the mentioned system identification technique, a valid model for the first 6 modes is identified, the frequency response of which is shown in Figure 5. The structural frequencies for the structure are $\omega_1 = 44.85$ Hz, $\omega_2 = 83.68$ Hz, $\omega_3 = 118.4$ Hz, $\omega_4 = 161.6$ Hz, $\omega_5 = 167.6$ Hz and $\omega_6 = 237.2$ Hz.

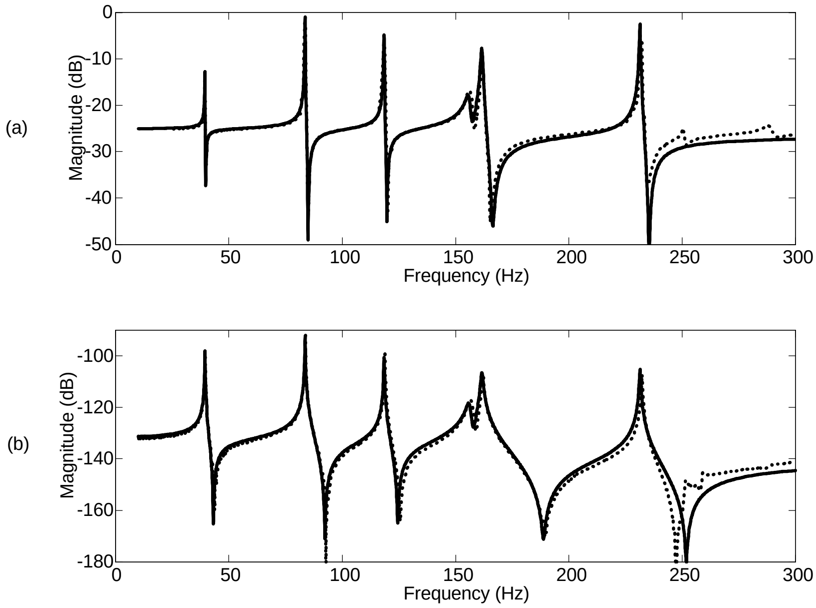

Figure 5. Frequency response (a) $|G_{vv}(s)|$ and (b) $|G_{dv}(s)|$, for the piezoelectric laminated plate bounded structure. Experimental data ($\cdots$) and model obtained using subspace based system identification (—).

*A Matlab implementation of this algorithm is freely available by contacting the corresponding author or by visiting http://rumi.newcastle.edu.au.

The following two subsections consider both a single mode and multiple mode robust shunt controller. Simulations are carried out for both cases. Each is then verified experimentally on the piezoelectric laminated plate.

4.1. Single Mode Robust Shunt Controller

For the single mode case, we will consider damping the second mode of the piezoelectric laminated plate structure. In Figure 6 (a), we apply a single mode controller to ω_2, or alternatively $\hat{\omega}_{2,0}$, as described in Moheimani et.al..[18] Next, two additional controllers are applied to the side lobes $\hat{\omega}_{2,-1}$ and $\hat{\omega}_{2,1}$, as shown in Figures 6 (b) and (c). The impedance required to damp the second mode, is

$$Z_1(s) = \frac{1-\beta_2}{C_p s \beta_2}, \tag{20}$$

where

$$\beta_2 = \frac{\alpha_{2,-1}\hat{\omega}_{2,-1}^2}{s^2 + 2\hat{d}_{2,-1}\hat{\omega}_{2,-1}s + \hat{\omega}_{2,-1}^2} + \frac{\alpha_{2,0}\hat{\omega}_{2,0}^2}{s^2 + 2\hat{d}_{2,0}\hat{\omega}_{2,0}s + \hat{\omega}_{2,0}^2} + \frac{\alpha_{2,1}\hat{\omega}_{2,1}^2}{s^2 + 2\hat{d}_{2,1}\hat{\omega}_{2,1}s + \hat{\omega}_{2,1}^2}.$$

Note, that $\alpha_{2,-1} = \alpha_{2,0} = \alpha_{2,1} = \frac{1}{3}$ and the chosen circuit parameters are tabulated in Table 1.

In order to achieve good performance, appropriate values for the damping parameters $\hat{d}_{2,-1}$, $\hat{d}_{2,0}$ and $\hat{d}_{2,1}$ need to be determined. The following optimization problem for the damped system could be solved:

$$D^* = \arg\min_{D>0} \left\| \hat{G}_{dv}(s) \right\|_2 \tag{21}$$

where $D^* = \{\hat{d}_{2,-1}, \hat{d}_{2,0}, \hat{d}_{2,1}\}$. The above optimization problem minimizes the H_2 norm of the damped transfer function from input disturbance voltage $v_{in}(s)$, to the displacement at a point on the structure $d(s)$. The optimization problem was solved for a number of initial guesses, and a solution was found; $\hat{d}_{2,-1} = 0.0110$, $\hat{d}_{2,0} = 0.0101$ and $\hat{d}_{2,1} = 0.0098$.

Simulated results for the $|G_{dv}(s)|$ and $\left|\hat{G}_{dv}(s)\right|$ show that the peak amplitude has been considerably reduced, as shown in Figure 6 (c).

Parameters	Sim. Value	Exp. Value
$\hat{\omega}_{2,-1}$	82.28 Hz	82.92 Hz
$\hat{\omega}_{2,0}$	83.68 Hz	83.58 Hz
$\hat{\omega}_{2,1}$	85.21 Hz	85.51 Hz

Parameters	Sim. Value	Exp. Value
$\hat{d}_{2,-1}$	0.0110	0.0150
$\hat{d}_{2,0}$	0.0101	0.00564
$\hat{d}_{2,1}$	0.0098	0.00245

Table 1: Single mode circuit parameters for the plate bounded structure.

To validate the proposed multiple mode robust shunt controller, the above impedance (20) and parameters listed in Table 1, is applied to the plate structure using the synthetic impedance.[22,23] When fine-tuning the proposed impedance parameters, it was found to be very sensitive, making the tuning process very time consuming.

From Figure 7, we can conclude that the proposed single mode robust shunt controller experimentally agrees with simulated results.

Aside, it should be noted that the proposed robust shunt controller could be immune to variations in structural dynamics. This contrasts to previous passive shunt techniques,[2,8–10] which are generally sensitive to variations in the structural frequencies. This was verified by shifting the simulated resonance frequencies ±1 Hz from their original values. Simulated results in Figure 8, employing the impedance (20), show that the performance of the system is not severely deteriorated by perturbing the resonance frequencies.

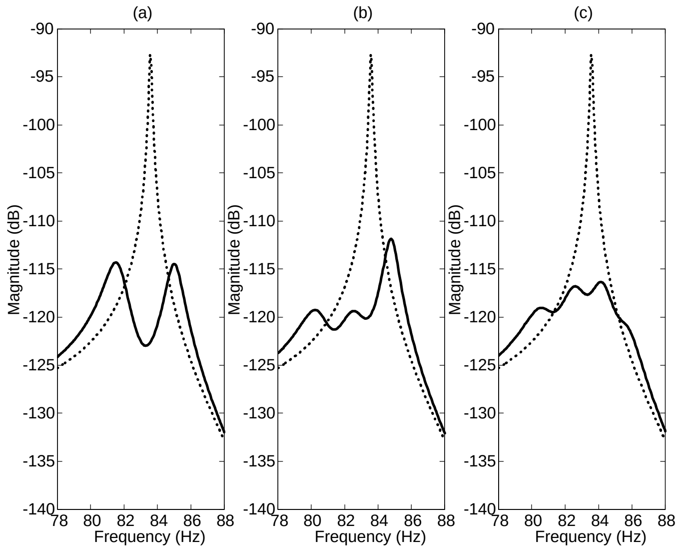

Figure 6. Simulated undamped $|G_{dv}(s)|$ ($\cdots$) and damped response $\left|\hat{G}_{dv}(s)\right|$ (—). Subfigure (a) original single mode controller applied to $\uparrow_{2;0}$, (b) second controller is applied to $\uparrow_{2;-1}$ and (c) third controller is applied to $\uparrow_{2;1}$.

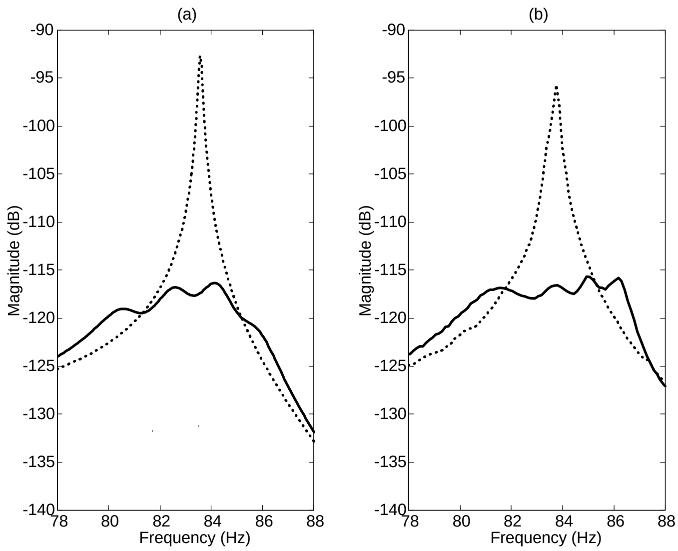

Figure 7. Subfigure (a) simulated results, and (b) experimental results. Undamped $|G_{dv}(s)|$ ($\cdots$) and damped response $\left|\hat{G}_{dv}(s)\right|$ (—).

4.2. Multiple Mode Robust Shunt Controller

For the multiple mode case, we will consider damping the 2nd and 3rd structural modes, i.e. $\omega_2 = 83.68$ Hz and $\omega_3 = 118.4$ Hz. Using the same procedure as suggested in Section 4.1, we will apply three additional controllers to the 3rd mode. That is, we require the following impedance:

$$Z_1(s) = \frac{1 - \beta_{23}}{C_p s \beta_{23}}; \tag{22}$$

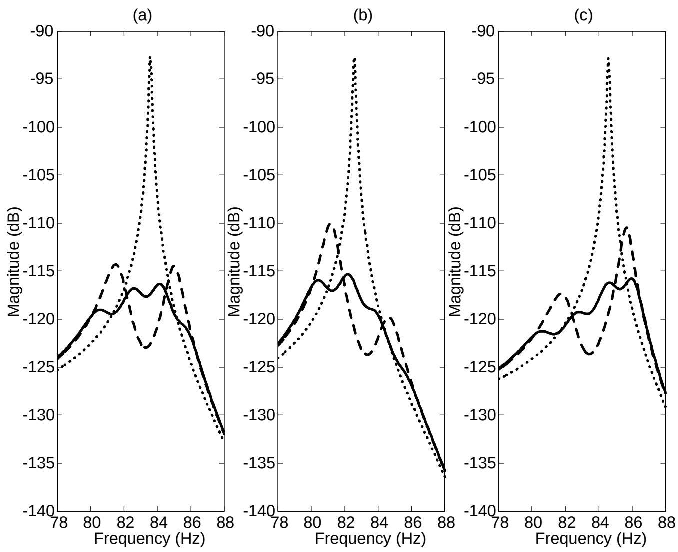

Figure 8. Simulated response: (a) original system, (b) poles moved -1 Hz from the original system, and (c) poles moved +1 Hz from the original system. Undamped system $|G_{wv}(s)|$ ($\cdots$), original single mode controller as described in Moheimani et.al.[18] (- - -) and proposed robust shunt controller (—).

where

$$\bar{\ }_{23} = \frac{\alpha_{2;-1}\omega_{2;-1}^2}{s^2 + 2\hat{\zeta}_{2;-1}\omega_{2;-1}s + \omega_{2;-1}^2} + \frac{\alpha_{2;0}\omega_{2;0}^2}{s^2 + 2\hat{\zeta}_{2;0}\omega_{2;0}s + \omega_{2;0}^2} + \frac{\alpha_{2;1}\omega_{2;1}^2}{s^2 + 2\hat{\zeta}_{2;1}\omega_{2;1}s + \omega_{2;1}^2} + \cdots$$
$$\frac{\alpha_{3;-1}\omega_{3;-1}^2}{s^2 + 2\hat{\zeta}_{3;-1}\omega_{3;-1}s + \omega_{3;-1}^2} + \frac{\alpha_{3;0}\omega_{3;0}^2}{s^2 + 2\hat{\zeta}_{3;0}\omega_{3;0}s + \omega_{3;0}^2} + \frac{\alpha_{3;1}\omega_{3;1}^2}{s^2 + 2\hat{\zeta}_{3;1}\omega_{3;1}s + \omega_{3;1}^2}.$$

Note that $\sum_{i=2}^{3}\sum_{i=-3}^{3}\alpha_{i;j} = 1$ for $\alpha_{i;j} > 0$, and $\alpha_{2;-1} = \alpha_{2;0} = \alpha_{2;1} = \alpha_{3;-1} = \alpha_{3;0} = \alpha_{3;1} = \frac{1}{6}$.

Parameters	Sim. Value	Exp. Value (Hz)
$\omega_{2;-1}$	82.2 Hz	81.95 Hz
$\omega_{2;0}$	83.4 Hz	83.27 Hz
$\omega_{2;1}$	84.6 Hz	84.09 Hz
$\omega_{3;-1}$	117.0 Hz	116.12 Hz
$\omega_{3;0}$	118.4 Hz	118.03 Hz
$\omega_{3;1}$	119.6 Hz	119.55 Hz

Parameters	Sim. Value	Exp. Value
$\hat{\zeta}_{2;-1}$	0.0091	0.00458
$\hat{\zeta}_{2;0}$	0.0084	0.00374
$\hat{\zeta}_{2;1}$	0.0079	0.00123
$\hat{\zeta}_{3;-1}$	0.0074	0.00515
$\hat{\zeta}_{3;0}$	0.0069	0.00864
$\hat{\zeta}_{3;1}$	0.0062	0.00451

Table 2: Multiple mode circuit parameters for the plate bounded structure.

Simulated results for the multiple mode robust shunt controller, undamped $|G_{dv}(s)|$ and damped $\left\|\hat{G}_{dv}(s)\right\|$ response, show that the structural amplitude has been considerably reduced, as shown in Figure 9. For our case, three individual controllers were applied to the 2nd and 3rd modes. It should also be noted that more then three additional controllers can be applied to each individual mode.

Using the synthetic impedance[22, 23] and the circuit parameters listed in Table 2, the impedance (22) is applied experimentally to the plate structure. From Figure 10 an amplitude reduction of approximately 16 dB for the 2nd and 3rd modes is observed.

From simulated and experimental results, we can conclude that the proposed multiple mode robust shunt controller is an effective method for shunt damping.

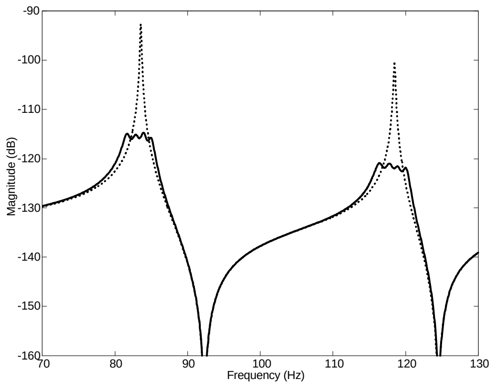

Figure 9. Simulated multiple mode robust shunt damping. Undamped $|G_{dv}(s)|$ (···) and damped $\left|\hat{G}_{dv}(s)\right|$ (—) response.

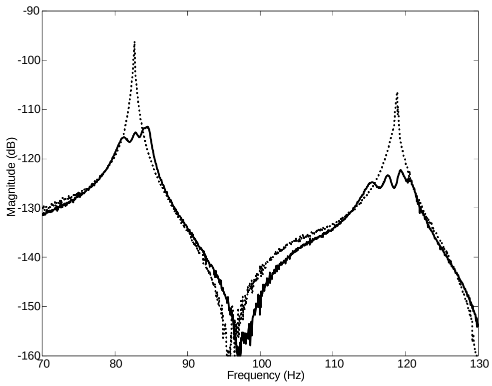

Figure 10. Experimental multiple mode robust shunt damping. Undamped $|G_{dv}(s)|$ (···) and damped $\left|\hat{G}_{dv}(s)\right|$ (—) response.

5. CONCLUSION

The robust piezoelectric shunt controller has been introduced as an alternate method of reducing structural vibrations. The effect of the robust piezoelectric shunt controller was studied theoretically and experimentally on a piezoelectric laminated plate structure. While achieving comparable performance to other passive control schemes, the proposed robust shunt controller has a number of advantages; it is robust, passive and can damp multiple modes. Preliminary results show that the proposed technique maybe less susceptible to environmental conditions than comparable techniques. Overall, the proposed technique is an effective method for damping structural modes but was considered to be experimentally time consuming.

6. ACKNOWLEDGMENTS

This research was supported by the Centre for Integrated Dynamics and Control (CIDAC) and the Australian Research Council (ARC).

REFERENCES

1. R. L. Forward, "Electronic damping of vibrations in optical structures," Applied Optics 18, pp. 690–697, March 1979.
2. N. W. Hagood and A. Von Flotow, "Damping of structural vibrations with piezoelectric materials and passive electrical networks," Journal of Sound and Vibration 146(2), pp. 243–268, 1991.
3. D. L. Edberg, A. S. Bicos, C. M. Fuller, J. J. Tracy, and J. S. Fechter, "Theoretical and experimental studies of a truss incorporating active members," Journal of Intelligent Materials Systems and Structures 3, pp. 333–347, 1992.
4. S. Behrens and S. O. R. Moheimani, "Current ‡owing multiple mode piezoelectric shunt dampener," in Proc. SPIE Smart Materials and Structures, Paper No. 4697-24, pp. 217–226, (San Diego, CA), March 2002.
5. S. Behrens, S. O. R. Moheimani, and A. J. Fleming, "Multiple mode current ‡owing passive piezoelectric shunt controller," Accepted for Publication in: Journal of Sound and Vibration , 2002.
6. C. R. Fuller, S. J. Elliott, and P. A. Nelson, Active Control of Vibration, Academic Press, 1996.
7. G. S. Agnes, "Active/passive piezoelectric vibration suppression," in Proc. SPIE Smart Structures and Materials, Passive Damping, SPIE Vol. 2193, pp. 24–34, (San Diego, CA), May 1994.
8. N. W. Hagood and E. F. Crawley, "Experimental investigation of passive enhancement of damping for space structures," Journal of Guidance, Control and Dynamics 14(6), pp. 1100–1109, 1991.
9. S. Y. Wu, "Piezoelectric shunts with parallel R-L circuit for structural damping and vibration control," in Proc. SPIE Smart Structures and Materials, Passive Damping and Isolation, SPIE Vol.2720, pp. 259–269, March 1996.
10. S. Y. Wu, "Method for multiple mode shunt damping of structural vibration using a single PZT transducer," in Proc. SPIE Smart Structures and Materials, Smart Structures and Intelligent Systems, SPIE Vol.3327, pp. 159–168, (Huntington Beach, CA), March 1998.
11. J. J. Hollkamp and T. F. Starchville, "A self-tuning piezoelectric vibration absorber," in Proc. 35th AIAA/ASME/ASCE/AHS/ACS Structures, Structural Dynamics and Materials Conference, Paper 94-1790, (Hilton Head, NC), 1994.
12. J. Q. Sun, M. R. Jolly, and M. A. Norris, "Passive adaptive and active tuned vibration absorbers – a survey.," Trans. ASME Combined Anniversary Issue J. Mech. Design and J. Vibration Acoustics 117(B), pp. 234–242, 1995.
13. A. v. Flotow, A. Beard, and D. Bailey, "Adaptive tuned vibration absorbers: Tuning laws, tracking agility, sizing and physical implementations," in Proc. Noise-Con '94, 1994.
14. A. J. Fleming and S. O. R. Moheimani, "Adaptive piezoelectric shunt damping," IOP Smart Materials and Structures 12, pp. 36–48, January 2003.
15. S. Behrens, "Passive and semi-active vibration control of piezoelectric laminates," Master's thesis, University of Newcastle, Australia, April 2001.
16. J. J. Dosch, D. J. Inman, and E. Garcia, "A self-sensing piezoelectric actuator for collocated control," Journal of Intelligent Material Systems and Structures 3, pp. 166–185, January 1992.
17. B. Ja¤e, W. R. Cook, and H. Ja¤e, Piezoelectric Ceramics, Academic Press, 1971.
18. S. O. R. Moheimani, A. J. Fleming, and S. Behrens, "On the feedback structure of wideband piezoelectric shunt damping systems," IOP Smart Materials and Structures 12, pp. 49–56, January 2003.
19. S. Moheimani and S. Behrens, "Multi-mode piezoelectric shunt damping with a highly resonant impedance," in Proc. IEEE International Conference on Control Applications, pp. 1132 –1137, (Glasgow, Scotland), September 2002.
20. S. Behrens, A. J. Fleming, and S. O. R. Moheimani, "A broadband controller for shunt piezoelectric damping of structural vibration," IOP Smart Materials and Structures 12, pp. 18–28, January 2003.
21. P. Van Overschee and B. De Moor, "Continuous-time frequency domain subspace system identi…cation," Signal Processing 52, pp. 179–194, 1996.
22. A. J. Fleming, S. Behrens, and S. O. R. Moheimani, "Synthetic impedance for implementation of piezoelectric shunt-damping circuits," Electronics Letters 36, pp. 1525–1526, August 2000.

23. A. Fleming and S. O. R. Moheimani, "Improved current and charge amplifiers for driving piezoelectric loads, and issues in signal processing design for synthesis of shunt damping circuits.," Journal of Intelligent Material Systems and Structures , Submitted August 2002.